Case Studies in Engineering Failure Analysis 7 (2016) 41–49

Contents lists available at ScienceDirect

Case Studies in Engineering Failure Analysis

journal homepage: www.elsevier.com/locate/csefa

Case study

Investigation of a Columbus, Ohio train derailment caused by fractured rail

Frank Zakar, Erik Mueller *

National Transportation Safety Board, Materials Laboratory Division, L'Enfant Plaza East, SW, Washington, DC 20594, United States

ARTICLE INFO

Article history:
Received 8 March 2016
Received in revised form 31 March 2016
Accepted 4 April 2016
Available online 11 April 2016

Keywords:
Rail
Tank car
Failure analysis
Fatigue
Derailment
Transverse detail fracture

ABSTRACT

On July 11, 2012 an eastbound Norfolk Southern train derailed 17 cars within the city limits of Columbus, OH. Three of the cars that derailed were carrying over 86,000 gallons of denatured ethanol. Once breached, the ethanol in the tank cars ignited, fueling a large fire. The derailment led to the evacuation of over 100 people and cost over $1.2 million. This paper will detail the on-scene response and failure analysis performed by the NTSB Materials Laboratory, focusing on the recovered rail that contained 25 transverse detail fractures.

1. Introduction

The National Transportation Safety Board (NTSB) is an independent United States federal government agency charged with determining the probable cause of transportation accidents, promoting transportation safety, and assisting victims of transportation accidents and their families. On July 11, 2012 at 2:03 a.m., eastern standard time, an eastbound Norfolk Southern Railway Company (NS) train derailed 17 cars within the city limits of Columbus, OH at a curve in the track. No train crewmembers sustained injuries. However, two citizens in the area sustained minor burn injuries. Approximately 100 people were evacuated from an area of 1 mile surrounding the derailment.

The train consisted of 2 locomotives, 97 loaded cars, and 1 empty car. The 3rd through the 19th cars derailed. Of the cars that derailed, three (positions 12 through 14) containing denatured ethanol breached, released product, and caught fire. The derailment and ensuing fire destroyed both main tracks of the line. The railroad estimated the damage at over $1.2 million [1].

During the on-scene investigation, multiple fractured rail segments were transported from the derailment site to a separate location within the Ohio State Fairgrounds for preliminary examination. Thirty-five rail pieces were recovered from the derailment area, several of which were attached to each other by joint bars. Of the pieces recovered, 24 of the exposed fracture faces exhibited transverse detail fractures, progressive fractures that originate at or near the surface of the rail head. Three of these rail fragments were transported to the NTSB Materials Laboratory in Washington, DC for additional examination.

Fractured rail has been studied extensively, with many fractures due to contact fatigue from rolling wheels of passing trains [2,3]. Besides the primary loading on the rail, secondary loading from thermal and residual stresses [4], as well as

* Corresponding author. Tel.: +1 2025916359.
E-mail address: erik.m.mueller@gmail.com (E. Mueller).

http://dx.doi.org/10.1016/j.csefa.2016.04.001

environmental changes such as temperature, strongly influence the likelihood of track failures [5]. Wheel-rail contact is only one of a variety of loading conditions requiring complicated long-term studies to determine appropriate life and inspection limits of rail under service [6].

The rail industry has classified rail defects and failures with nomenclature unique to the business [7]. Progressive fractures initiating at or near the rail surface, called detail fractures in North America, are denoted by the orientation relative to the rail rolling direction. Transverse detail fractures can initiate due to rolling contact fatigue failure modes such as shelling (a longitudinal separation of the rail head near the wheel running surface) and head checking (transverse cracking on the gage corner from excessive surface cold working). These failure modes are typical when shear stresses at the wheel-rail contact region exceed the limits for the rail steel. Detail fractures also initiate at internal defects in the rail from manufacturing flaws [8]. Understanding and detecting these and other failure mechanisms is important in preventing catastrophic derailments due to rail failure.

2. Investigation methods

The rail fragments were inspected using destructive and non-destructive methods by the NTSB Materials Laboratory. The on-scene parts were photographed using a Canon EOS Rebel T3i digital camera. This same digital camera was used in conjunction with a Keyence VHX-1000 digital microscope for laboratory documentation. The digital microscope was capable of producing high-dynamic range and composite high depth-of-field images.

Specimens excised from the rail fragments were examined using a Zeiss Auriga 40 field emission scanning electron microscope (SEM). This microscope was equipped with a Thermo Scientific UltraDry NORAN System 7 energy-dispersive X-ray spectroscopy (EDS) for inspection of chemical composition.

Several metallographic cross sections of the rail fragments were prepared. The cross sections were polished and etched with 4% Nital. These metallographic specimens were evaluated using a Zeiss Axio Observer Z1m inverted microscope.

Hardness testing was performed using a Wilson Rockwell hardness tester per ASTM E18 using a diamond indenter and 150 kg load to obtain Rockwell C (HRC) values [9]. The HRC hardness values were converted to Brinell (HB) values [10]. Specimens from the rail fragments were submitted to Lehigh Testing Laboratories in New Castle, DE for chemical analysis. The chemical compositions were inspected using inductively coupled plasma mass spectroscopy (ICP) as well as a combustion infrared detection of carbon and sulfur.

3. Results of the investigation

3.1. Columbus, OH on-scene investigation

Each rail piece was arbitrarily labeled with an identification number between "0" and "200" with each end marked "A" or "B." The ends of each recovered rail piece were documented as being joined to another rail with a joint bar, torch-cut in the field, or fractured. The total length of recovered pieces was approximately 272 ft.

The web portion of the rail pieces contained raised characters that identified the size, date, and manufacturer of the rail. The markings on the rail fragments were consistent with manufacture by three different steel mills:

- US Steel in February 1979 and September 1981.
- Bethlehem Steelton in September 1981.
- Colorado Fuel and Iron in December 1988.

According to the American Railway Engineering Association (AREA) specifications applicable at time of manufacture of the above rail segment, the markings identified the rail to be 132 pound-per-yard rolled steel [11]. The American Railway Engineering and Maintenance-of-Way Association (AREMA) was formed from the merger of the American Railway Bridge and Building Association, Communications and Signal Division of the Association of American Railroads, and the Roadmasters and Maintenance of Way Association with AREA in 1997, which now administers the specifications for rail manufacture. The rail pieces from the three mills contained the "CC" mark indicating that the steel was control cooled, a practice used to reduce hydrogen accumulation in the rail and to prevent internal flake formation [12]. The development of hydrogen flakes during steel manufacture has been shown to cause premature fracture [13].

By visual inspection, many of the running surfaces of the head portions for the rail pieces showed evidence of shelling and severe rolling-contact fatigue cracks, consistent with head checking [14]. Many of the fracture surfaces contained transverse detail fractures that extended from the gage side (inward surface facing the wheel flange) of the rail head in areas that coincided with observed head checking, as shown in Fig. 1.

Transverse detail fractures typically exhibit a smooth texture and dark tinted region relative to other areas on the fracture surface, consistent with fatigue cracking in the rail head [7,14]. In this case, the dark tinted portions of the fracture surfaces appeared black or dark brown, consistent with iron oxide on the surface of steel. The area within the detail fracture portions exhibited crack arrest marks consistent with progressive cracking, later determined to be fatigue [15]. The areas located outside of the transverse detail fracture showed light gray coarse granular features consistent with overstress fracture

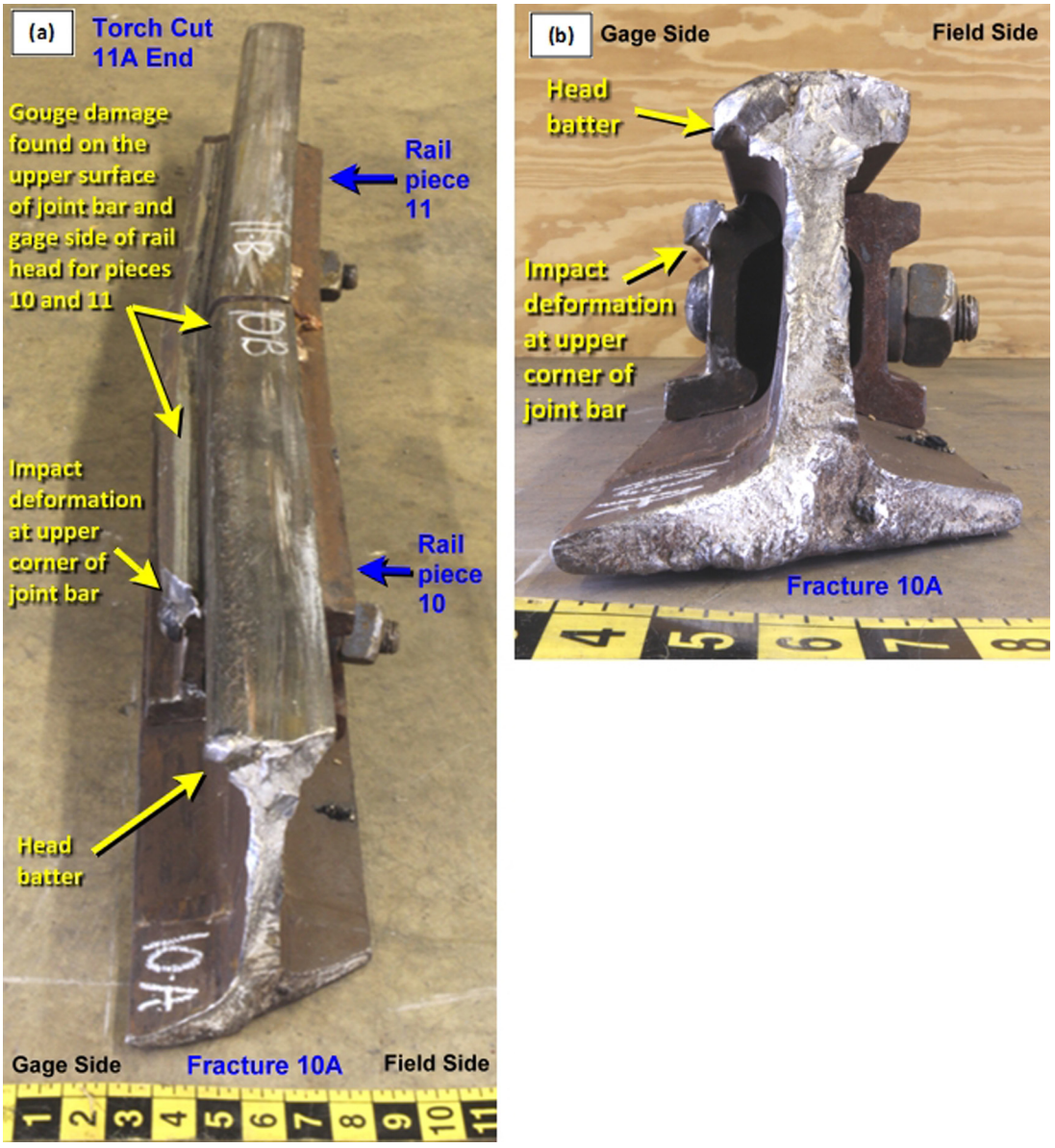

Fig. 1. Rail samples 10 and 11 showing (a) the fracture face 10A end and (b) a close-up photograph of the fracture face 10A.

[16]. Twenty-four transverse detail fractures were identified on site. The remaining rail fractures exhibited features consistent with overstress. Three of the rail fragments with transverse detail fractures (samples "10", "80", and "130") were examined further at the NTSB Materials Laboratory:

- Sample "10" (approximately 56 in. long that was battered on the "A" end). Rail piece 10 was attached to rail piece 11 by a pair of joint bars.
- Sample "80" (approximately 10 in. long) contained the largest transverse detail fracture.
- Sample "130" (approximately 27 in. long) contained a crack on the running surface of the head.

3.2. Materials laboratory investigation

The fracture face of one of the rail sample 10 (labeled "10A") exhibited mechanical damage that had obliterated many of the features on the fracture surface. The running surface of the head and the gage side exhibited batter deformation, as

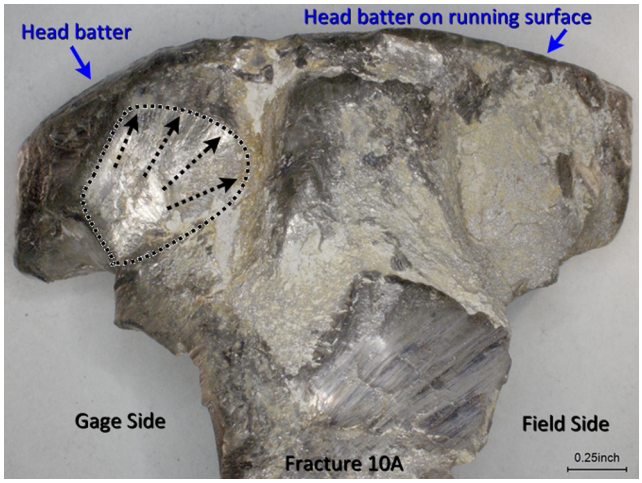

Fig. 2. Fracture face 10A excised from rail sample 10, after cleaning. The dashed circled area outlines the detail fracture (propagating in the direction of the arrows) that was present on the battered fracture surface.

shown in Fig. 1. The joint bar on the gage side of the rail showed evidence of impact damage that corresponded to fracture end 10A. The same joint bar had been gouged along its entire length. This corresponded with gouging found on the gage side of rail pieces 10 and 11.

Fracture surface 10A was sectioned from the rest of the rail by a cross sectional cut approximately 1 in. from the fracture and subjected to extensive cleaning. As shown in Fig. 2, the head portion contained a smooth flat plane with coarse radial marks that ran from left to right. This area contained crack arrest marks consistent with a progressive fracture that extended from the gage side of the head (making this the 25th transverse detail fracture discovered in the investigation).

The head portions of rail samples 80 and 130 exhibited surface flaking and head checking on the running surfaces (see Figs. 3 and 4). The gage side of the head from samples 80 and 130 exhibited shell cracks that extended from the upper corner of the head. The surface below the open shell cracks contained shallow horizontal cracks.

Fracture face 80A from sample 80, which exhibited the largest transverse detail fracture, extended approximately 2.5 in. below the running surface of the head into the web. This detail fracture encompassed approximately 70% of the worn rail head (see Fig. 5), calculated as a percentage of the remaining head cross section [17]. The next largest transverse detail fracture, found on fracture face 80B, encompassed approximately 30% of the worn rail head. Of the 24 exposed fracture faces exhibiting transverse detail fractures, the size of the transverse detail fractures on the worn head portion of the rail pieces ranged between approximately 1 and 70%.

Rail sample 130 contained an additional crack that extended between the head and the lower end of the web portion, as shown in Fig. 4. In the laboratory, the ends of the rail were subjected to a bending stress to intentionally overstress the rail,

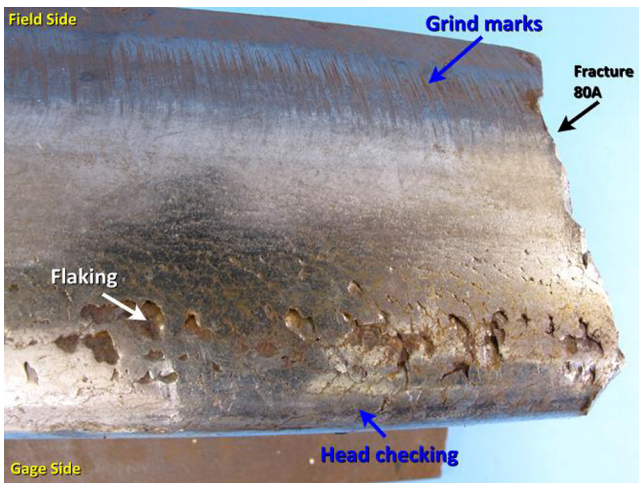

Fig. 3. The running surface of rail sample 80, showing the damage on the head adjacent fracture surface 80A. The flaking indicated in the figure refers to shallow features in the metal surface that separated from the gage corner of the rail head.

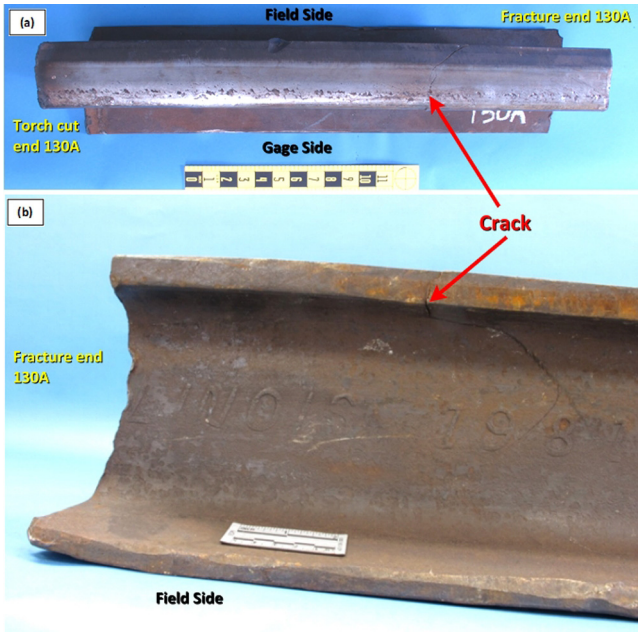

Fig. 4. Rail sample 130 from (a) running surface of the head and (b) the field side. The upper corner of the head on the gage side contained shell crack. An internal crack was visible on both the running surface and the field side of the web.

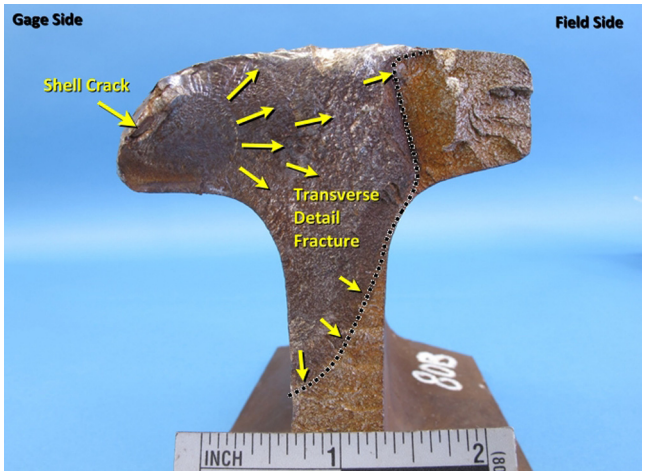

Fig. 5. Fracture surface 80A from rail sample 80, showing a transverse detail fracture that extended into the web portion from an open shell crack in the upper corner of the head.

exposing the crack faces. Fig. 6 shows one of the mating fracture surfaces of the opened crack, revealing a subsurface fatigue crack located on the gage side of the head.

Transverse cross sections, which included the head, web, and base portion, were cut from the rail comprising samples 10, 11, 80, and 130. Fig. 7 illustrates an as-manufactured 132 pound/yard rail profile superimposed over the rail cross section. The superimposed image in Fig. 7 shows the amount of the head wear (approximately 29%).

The height of the rail was measured at the center of the rail between the upper (running) surface of the head and the lower surface of the base using a digital height gage on a granite table [11]. Table 1 shows the measured height of rail pieces 10, 11, 80, and 130. The table lists the amount of vertical wear in the head portion (calculated as height difference between as-manufactured and the accident rail), vertical head wear limit (specified by NS when rail replacement is recommended), and wear vertical limit when a slow order was required. A slow order requires passing trains to operate at a reduced speed until the worn rail is replaced. For service conditions under which this train was operating, the slow order stated not to exceed 25 mph. The derailment occurred on a main track that was designated as Federal Railroad Administration Class 2 track, with a maximum authorized speed of 25 mph. NTSB investigators found that the train's event recorder data indicated the train was moving at 25 mph immediately prior to the derailment, which did not exceed the slow order restriction.

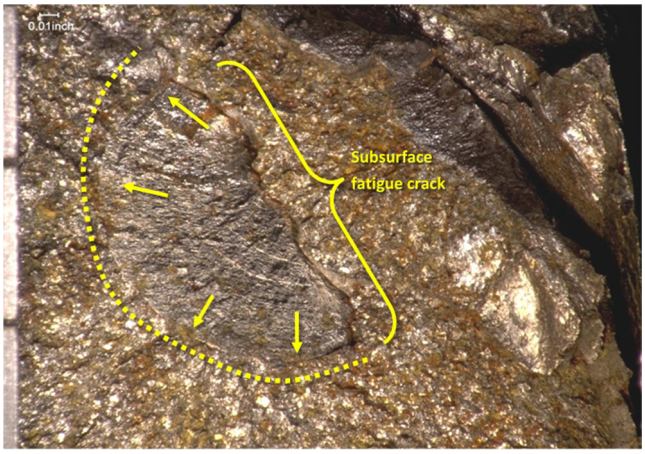

Fig. 6. The exposed fracture from the intentionally opened crack in Fig. 4, showing a subsurface fatigue crack on the gage side of the head of sample 130.

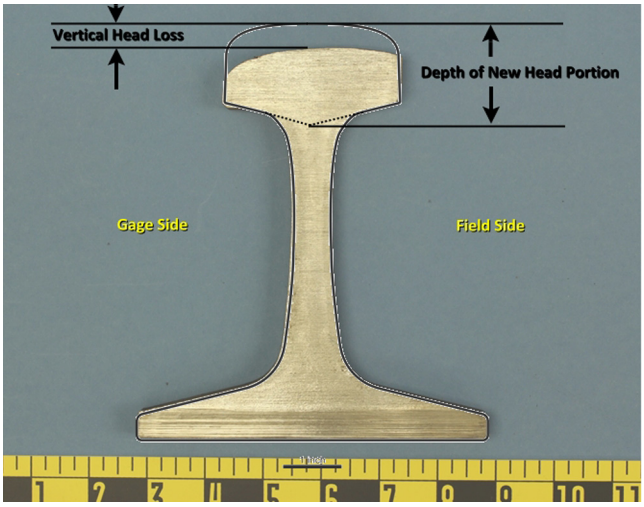

Fig. 7. Cross section of rail sample 10, 1 in. from fracture surface 10A, superimposed against the profile of new 132 pound/yard rail (indicated by black outline). The amount of vertical head loss for this piece was calculated to be approximately 29% relative to a new head.

Table 1
Vertical wear measurements for rail fragments, compared with prescribed limits (132 pound rail).

Rail piece	Specified height for new rail (in.)	Measured height of service rail (in.)	Difference between new and service rail (in.)	NS vertical wear limit[a] (in.)	Do measurements exceed NS vertical wear limits?	When does NS require a slow order for worn rail?[b]	Require NS slow order?
10	7 1/8	6.62–6.67	0.46–0.51	Greater than	Yes	Greater than	No
11	(7.125)	6.81–6.87	0.26–0.32	7/16 (0.4375)	No	9/16 in.	No
80		6.57–6.63	0.50–0.56		Yes	(0.5625 in.)	No
130		6.64–6.67	0.46–0.49		Yes		No

[a] When operating on main track 20 million gross tons (MGT) and curve is greater than 5°, rail is recommended for replacement (listed for future replacement) when vertical wear is greater than 7/16 in.
[b] When operating between 5 and 20 MGT and lateral (side) wear is greater than 9/16 in., trains are to be put into slow ordered until rail is replaced.

The measured vertical head wear for rail samples 10, 80, and 130 was greater than the vertical wear limit specified by NS [18]. According to the results of the measurements and NS standards, these rail pieces would have been listed for future replacement. However, the vertical wear for the four rail pieces (10, 11, 80, and 130) was less than would have been required for a slow order. The lateral wear on the heads was also measured, but none exhibited wear in excess of the NS limits.

A head portion of each rail cross section was cut from the web portion. These portions were ground, polished, and etched. Examination of the etched sections revealed the head portion of rail piece 11 contained a lighter etched area between the

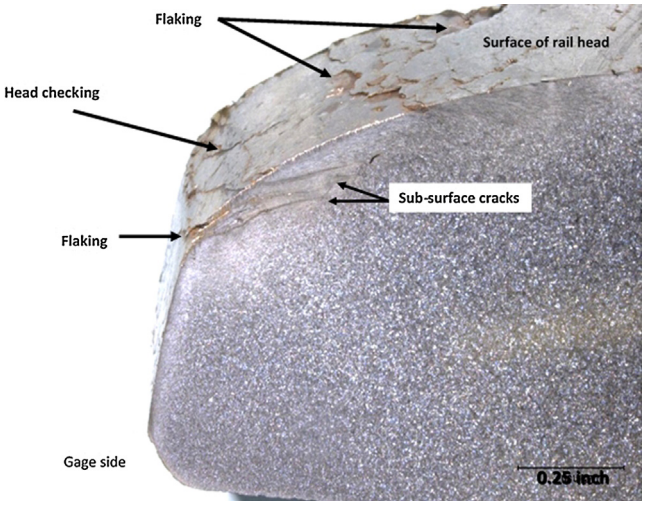

Fig. 8. Optical metallography of a cross section of the head of sample 130, showing the upper corner of the head on the gage side angled to view running side damage and prepared face. Sub-surface cracks extended from flaking areas (4% Nital etch, bright field).

web and head portion. This microstructure was typical for "high strength rail" where the head was hardened by induction heating, consistent with a finer grain size [19]. The head portion of the remaining cross-sectioned rail pieces showed a uniform pearlite grain structure across the head, a microstructure consistent with "standard rail" [20]. The running surface of each head cross section contained a thin layer of metal flow consistent with mechanical deformation. The upper corners of the head contained subsurface cracks that extended from the shelled and highly-deformed areas (Fig. 8). There were no indications inclusions or untempered martensite in the polished and etched cross sections.

According to the applicable AREA specifications at the time, rail manufactured between 1979 and 1988 were designated as "standard rail" or "high strength rail." "Standard rail" manufactured at the time specified minimum hardness of 285 HB for the head; "high strength rail" had specified hardness between 321 HB and 388 HB for the head [11].

Transverse hardness measurements were made laterally between the field side (original surface) and core of the rail head. Another set of traverse hardness measurements were made vertically along the centerline of the rail heads that extended between the running worn surface and bottom portion of the head. The hardness values for the head portion of rail pieces 80 and 130 were consistent with hardness values for "standard rail." The hardness values for the head portion of the Colorado Fuel and Iron rail piece 11 was consistent with hardness values for "high strength rail."

Fracture face 10A contained a transverse detail fracture that was located approximately 1 in. away from an electric flash butt weld. A section was made through the electric flash butt weld that was polished and etched. The edge of the heat affected zone (HAZ) was located approximately 0.75 in. from the fusion line. The fusion line showed no evidence of weld defects. The hardness at the weld was 300 HB (29 HRC), increasing to a maximum of 321 HB (32 HRC) at the approximate location of the transverse detail fracture, and then tapering to 267 HB (24 HRC) at the edge of the heat-affected zone. The hardness increased in the base metal to an average of 286 HB (27 HRC).

The head portion of the rail pieces was submitted for chemical analysis. The chemical analysis for rail pieces 10, 80, and 130 were consistent with the prescribed specification for "standard rail," similar to AISI 1580 carbon steel. The chemical analysis for rail piece 11 was consistent with the prescribed specification for "high strength rail" [11].

4. Analysis and discussion

Derailment of rail cars was likely caused by a transverse detail fracture that emanated from the upper corner of the head on the gage side of a rail. The track in the derailment area contained 25 transverse detail fractures. All the transverse detail fractures had initiated in the upper corners on the gage sides of the rail heads. The origin of many of the transverse detail fractures was open shell cracks.

Rail head batter on one of the fracture faces (labeled 10A) was consistent with damage incurred by train wheels running over the separated segment after fracture of the rail head. Since no other rail pieces showed evidence of similar batter damage, fracture face 10A was most likely the point of derailment. Even though the battered fracture surface may not contain the largest or oldest fatigue crack, the batter indicates that this section of rail fell out of alignment first.

Because of the post-fracture batter damage to fracture face 10A, the extent of damage prior to the derailment could not be determined. Even without the damage, determining the time of fatigue crack propagation is often speculative. This is due to the non-uniform loading typically seen by rails in service. Individual rails are often unevenly supported by rail ties, ballast, and sub-ballast. These supports can change over time due to service and weather conditions. Furthermore, the freight car and locomotive weight supported by the rail varies significantly.

At the request of the NTSB, Volpe National Transportation Systems Center (U.S. Department of Transportation) studied the defect size of the transverse detail fracture at the time of the last rail inspection [21]. The analysis estimated that the size of the transverse detail fracture on fracture face 80B at the time of the last inspection was between 10.1 and 11.2% of the head area. The addition of severe head wear can accelerate the propagation rate of a detail fracture in rail heads [22]. The severity of wear, amount of head checking, and therefore fatigue damage has been found to increase as the radius in curvature in the rail decreases [23,24]. The location of this derailment was at a curve in the track. These fatigue cracks generally do not require metallurgical defects to initiate [24].

The probability of detection increases as the size of the crack increases. AREMA currently provides guidance on crack probability of detection (which was reported as reliability ratio) [25]. For a crack between 10% and 20% of the head area, the probability of detection on the first round of inspection would have been about 65%. The size of transverse detail fracture for fracture face 80B was in this range. Because detail fractures may not be detected on the first round of inspection, more frequent inspections are often performed on rail expected to have detail fractures in combination with severe head wear.

This accident demonstrates that detail fractures in worn rail heads operating under heavy yearly tonnage will continue to grow, even when the trains are operating on a slow order, as discussed in a previous study [26].

Conclusions

The National Transportation Safety Board determined the probable cause of this accident was a broken rail that exhibited evidence of rolling contact fatigue.

While no recommendations were developed specifically from this accident, the NTSB did reiterate previous safety recommendations [27]. These recommendations stated for the railroad companies to

- Review all internal rail defect detection procedures to eliminate exceptions.
- Develop inspection and maintenance programs based on damage-tolerance programs to identify and remove internal defects before reaching critical size.
- Use methods that accurately measure rail head wear.

Acknowledgements

In accordance with Title 5 Code of Federal Regulations §2635.807(b)(2), the views expressed in this article do not necessarily represent the views of the National Transportation Safety Board or the United States Government.

The authors would like to thank David Jeong at the Volpe National Transportation Systems Center (U.S. Department of Transportation) for performing the defect calculation study for this investigation.

References

[1] National Transportation Safety Board Accident. Railroad accident brief report no. RAB1408. Investigation DCA12MR006; 2012, July 11.
[2] Thompson AW, Albert DE, Gray III . Fatigue crack growth in rail steels. In: Rail quality and maintenance for modern railway operation. 1993;p. 361–72.
[3] Grigorovich KV, Trushnikova AS, Arsenkin AM, Shibaev SS, Garber AK. Structure and metallurgical quality of rail steels produced by various manufacturers. Russ Metall (Metally) 2006;5(September–October):427–38.
[4] Ravaee R, Hassani A. Fracture mechanics determinations of allowable crack size in railroad rails. J Fail Anal Prev 2007;7:305–10.
[5] Edel KO. Allowable crack sizes for railway wheels and rails. Theor Appl Fract Mech 1988;9:75–82.
[6] Orringer O, Tang YH, Gordon JE, Jeong DY, Morris JM, Perlman AB. Crack propagation life of detail fractures in rails. DOT/FRA/ORD-88/13 DOT-TSC-FRA-88-1. Washington, DC: US Dept. of Transportation; 1988.
[7] Sperry Rail Service. In: Rail defect manual. Danbury, CT: Sperry Division of Automation Industries, Inc.; 1964.
[8] Tov GM, Vyaz'mina TM. Investigations of the fatigue and fractures of samples of rail steel by a fractographic method. Strength Mater 1976;8(January (1)):96–9.
[9] ASTM E18: standard test methods for Rockwell hardness and Rockwell superficial hardness of metallic materials. West Conshohocken, PA: ASTM International.
[10] ASTM E140: standard hardness conversion tables for metals relationship among Brinell hardness, Vickers hardness, Rockwell hardness, superficial hardness, Knoop hardness, scleroscope hardness, and Leeb Hardness. West Conshohocken, PA: ASTM International.
[11] American Railway Engineering Association. Rail. In: Manual for railway engineering. Chicago, IL: AREA; 1991 [chapter 4].
[12] Besedin PT. The causes of flake formation in steel. Met Sci Heat Treat Met 1959;1(February (2)):17–21.
[13] Aleksandrov IV, Kuznetsov EP, Boikov DV, Mogil'nyi VV, Zakharova TP. Improving rail-steel production. Steel Transl 2013;43(February (2)):69–72.
[14] Masumoto H, Sugino K, Nishida S, Kukihara R, Matsuyama S. Some features and metallurgical considerations of surface defects in rail due to contact fatigue ASTM STP 644. In: Stone , Knupp , editors. Rail steels—developments, processing, and use. 1978. p. 233.
[15] Sachs NW. Understanding the surface features of fatigue fractures: how they describe the failure cause and the failure history. J Fail Anal Prev 2005;5(2):11–5.
[16] Kerlins V, Phillips A. Modes of fracture. ASM handbook. Fractography, vol. 12. ASM International; 1987. p. 12–71.
[17] Federal Rail Administration. Track inspector rail defect reference manual; 2011;2.
[18] Norfolk Southern Railway. Rail wear limits. MW&S standard procedure 268; 2011.
[19] Wang L, Pyzalla A, Stadlbauer W, Werner EA. Microstructure features on rolling surfaces of railway rails subjected to heavy loading. Mater Sci Eng A 2003;359(October (1–2)):31–43.
[20] Wetscher F, Vorhauer A, Stock R, Pippan R. Structural refinement of low alloyed steels during severe plastic deformation. Mater Sci Eng A 2004;387–389(December):809–16.
[21] Jeong D, Perlman B. Back-calculation of defect size at time of last rail test for train derailment at Columbus, Ohio on July 11, 2012. Volpe National Transportation Systems Center, US Dept. of Transportation; 2012.

[22] Lyons ML, Jeong DY, Gordon JE. Fracture mechanics approach to estimate rail wear limits. In: Proceedings of the 2009 ASME Rail Transportation Fall Technical Conference; 2009. p. 137–46.
[23] Zhong W, Wang W, Liu Q. Study on fatigue crack behavior of rail in different curve radius. In: Advanced tribology. Berlin: Springer Berlin Heidelberg; 2010. p. 255–6.
[24] Eisenmann J, Leykauf G. The effect of head checking on the bending fatigue strength of railway rails. In: Rail quality and maintenance for modern railway operation. 1993;p. 425–33.
[25] American Railway Engineering and Maintenance-of-Way Association. Maintenance of rail. In: AREMA manual for railway engineering. Chicago, IL: AREMA; 2015 [chapter 4-4-1].
[26] Stone DH. Rail developments and requirements for heavy haul railways. In: Kalker , Cannon , Orringer , editors. Rail quality and maintenance for modern railway operation. 1993. p. 15–26.
[27] Safety recommendations R-08-9 through R-08-12. Washington, DC: National Transportation Safety Board; 2008, May 22.